

Multi-RIS Discrete-Phase Encoding for Interpath-Interference-Free Channel Estimation

Kamran Keykhosravi, *Member, IEEE*, and Henk Wymeersch, *Senior Member, IEEE*

Abstract—Reconfigurable intelligent surfaces (RISs) are one of the foremost technological enablers of future wireless systems. They improve communication and localization by providing a strong non-line-of-sight path to the receiver. In this paper, we propose a pilot transmission method to enable the receiver to separate signals arriving from different RISs and from the uncontrolled multipath. This facilitates channel estimation and localization, as the channel or its geometric parameters can be estimated for each path separately. Our method is based on designing temporal phase profiles that are orthogonal across RISs without affecting the RIS beamforming capabilities. We take into consideration the limited resolution of the RIS phase shifters and show that in the presence of this practical limitation, orthogonal phase profiles can be designed based on Butson-type Hadamard matrices. For a localization scenario, we show that with our proposed method the estimator can attain the theoretical lower bound even with one-bit RIS phase resolution.

Index Terms—Reconfigurable intelligent surfaces, analog beamforming, interference mitigation, Butson-type Hadamard matrices, channel estimation, localization.

I. INTRODUCTION

ONE of the most-promising emerging technologies in 6G communication systems are reconfigurable intelligent surfaces (RISs), which enable the control and optimization of the propagation channel, thereby enabling or boosting radio communication, localization, and sensing [1]. An RIS comprises a large number of passive elements, with sub-wavelength inter-element spacing. Each element scatters the impinging signal after applying a phase shift to it. In order to improve the communication quality-of-service (QoS) in a wireless network comprising one or more RISs, the RISs' phase profiles should be jointly optimized [2]. Performing such optimization requires the channel state information (CSI) for the channel corresponding to each individual RIS. Furthermore, in localization, parameter estimation for each of the controlled channels as well as the uncontrolled one is often essential. Obtaining the per-channel CSI entails resolving the interpath interference at the receiver (Rx), which is the topic of this paper. This task is challenging since *i*) unlike more conventional technologies such as relays, RISs are often passive and are not equipped with a radio-frequency (RF) chain, thus they cannot transmit, receive, process, or amplify signals [3] *ii*) RISs can only apply discrete phase shifts to the impinging signal [4].

Channel estimation for RIS-aided wireless systems has been studied in a number of papers (see [5, Sec. VI-G]). In order

to estimate the channel from an individual RIS, it is generally assumed that the uncontrolled multipath is blocked (see e.g., [6]) or that a RIS can be “switched off” (i.e., operate in absorption mode), thereby avoiding interpath interference (see e.g., [7]). In [8], [9], the channel for each RIS element is estimated by designing the RIS phase profile according to orthogonal sequences. In all these studies the wireless system is aided by a single RIS. A limited number of papers consider channel estimation in multi-RIS systems: in [10], channel estimation is performed for a multi-RIS multiple-input multiple-output (MIMO) system via successive hierarchical beam sweeping for each of the RISs. In [11] explicit multi-RIS channel estimation is bypassed by maximizing the achievable rate directly using a supervised learning technique.

Similarly as in channel estimation, in multi-RIS localization it has been considered switching off RISs to avoid interpath interference [12]. In [13], a semi-passive localization scenario has been studied, where each of the users are equipped with an RIS and orthogonal RIS phase profiles are used to resolve the interpath interference. Cramér-Rao lower bounds (CRBs) on the localization accuracy have been derived in [14] for multi-RIS MIMO systems, however no estimation method is provided. In [15] localization is performed via successive interference cancellation, assuming that the direct channel is much stronger than the channel reflected from an RIS.

In this paper, we tackle the problem of interpath interference during pilot transmission for a generic multi-RIS communication or localization scenario. Our specific contributions are as follows: *(i)* we design temporally coded RIS phase profiles with finite resolution, such that the signal received by different paths are mutually orthogonal, based on Butson-type Hadamard (BH) matrices; *(ii)* we show that these codes do not affect the chosen beamforming RIS phase profile, though they introduce a delay; *(iii)* to address the delay, we study the problem of finding the shortest orthogonal code for finite resolution RIS using properties of BH matrices; *(iv)* to assess the effectiveness of our proposal, we consider the semi-passive localization scenario in [13] under limited RIS phase shifts resolution and show that the CRB bounds can be obtained with one bit phase resolution, while ignoring the finite RIS phase resolution leads to significant interpath interference.

Notation: The vectors, which are columns by default, are represented by the lower-case bold letters and the matrices by the upper case bold ones. The i th element of vector \mathbf{x} is shown by $[\mathbf{x}]_i$ and the element on the i th row and j th column of matrix \mathbf{X} is shown by $[\mathbf{X}]_{i,j}$. Furthermore, $[\mathbf{X}]_i$ indicates the i th row of matrix \mathbf{X} . We show the the ceiling function by $\lceil \cdot \rceil$. We define the set \mathbb{T} to represent the circle group

This work was supported, in part, by the Swedish Research Council under grant 2018-03701 and the EU H2020 RISE-6G project under grant 101017011.

The authors are with Chalmers University of Technology, Department of Electrical Engineering, Sweden.

and \mathbb{T}_R to represent $\{e^{j2\pi r/R}\}_{r=0}^{R-1}$. The zero-mean circularly symmetric Gaussian distribution with covariance matrix \mathbf{C} is represented by $\mathcal{CN}(\mathbf{0}, \mathbf{C})$. The Kronecker and Hadamard products are indicated by \otimes and \odot respectively. We define $\mathbf{X}^{\otimes n} = \underbrace{\mathbf{X} \otimes \cdots \otimes \mathbf{X}}_{n \text{ times}}$ and $\mathbf{X}^{\otimes 0} = \mathbf{1}$.

II. SYSTEM MODEL

We consider a general MIMO scenario, where the transmitter (Tx) sends pilots with constant energy, for the purpose of channel estimation or user localization. The signal from the Tx is received via the uncontrolled multipath and controlled multipath from the $K \geq 1$ RISs. We ignore multi-bounce effects from two or more RISs. The received signal at t th transmission can be represented as

$$\mathbf{y}_t = \left(\mathbf{H}_0 + \sum_{k=1}^K \mathbf{H}_k(\gamma_{k,t}) \right) \sqrt{E_s} + \boldsymbol{\nu}_t. \quad (1)$$

Here, $\mathbf{H}_0 \in \mathbb{C}^{N_{\text{rx}} \times N_{\text{tx}}}$ represents the uncontrolled channel (which may or may not be blocked), where N_{rx} and N_{tx} are the Rx and Tx antenna count. The channel from Tx to the k th RIS to the Rx is shown by $\mathbf{H}_k(\gamma_{k,t})$, where $\gamma_{k,t} \in \mathbb{T}_R^{N_{\text{ris}}}$ represents the phase profile at time t of RIS k with N_{ris} being the number of unit cells per RIS and $R \in \mathbb{N}_{>1}$ being the RISs phase resolution. The transmitted pilots are assumed to identical to $\sqrt{E_s}$. Finally, $\boldsymbol{\nu}_t \sim \mathcal{CN}(\mathbf{0}, N_0 \mathbf{I}_{N_{\text{rx}}})$ represents the complex additive zero-mean white noise. The channel related to the k th RIS can be decomposed as

$$\mathbf{H}_k(\gamma_{k,t}) = \mathbf{H}_{\text{sr},k} \text{diag}(\gamma_{k,t}) \mathbf{H}_{\text{ts},k}, \quad (2)$$

where $\mathbf{H}_{\text{sr},k} \in \mathbb{C}^{N_{\text{rx}} \times N_{\text{ris}}}$ and $\mathbf{H}_{\text{ts},k} \in \mathbb{C}^{N_{\text{ris}} \times N_{\text{tx}}}$ represent the channels from RIS to Rx and from Tx to RIS, respectively. One can observe that for any $h \in \mathbb{T}_R$, we have

$$\mathbf{H}_k(h\gamma_{k,t}) = h\mathbf{H}_k(\gamma_{k,t}). \quad (3)$$

Finally, we assume that the system designer has chosen desired phase profile $\zeta_{k,q} \in \mathbb{T}_R^{N_{\text{ris}}}$ for each RIS k , for transmissions times $q \in \{0, \dots, Q-1\}$, $Q \geq 1$. The choice of $\zeta_{k,q}$ and Q is arbitrary, and could correspond, e.g., to Q different beams that are directed to the Rx (e.g., if some prior knowledge of the Rx position is available); or to cover a plurality of users; or random beams to provide omnidirectional illumination.

Our proposed design (see Section III) is applicable to all the channel models that can be described by (1)–(3), which includes most of the RIS channel models in the literature, whether narrow-band or wide-band, near-field or far-field, parametric or unstructured, single-RIS or multi-RIS, and with or without uncontrolled multipath.

III. RIS PHASE PROFILE DESIGN

A. Slow and fast RIS phase profiles

We design the RIS phase profile by dividing the total transmission time T , into P intervals with Q symbols, i.e., we set $T = P \times Q$. Here, P is a design parameters, which will be discussed later. We represent the RIS phase profile as

$$\gamma_{k,t} = \beta_{k,p} \zeta_{k,q}, \quad (4)$$

where $p = t \bmod P$ and $q = (t - p)/P$, so we have that $t = qP + p$. We call $\beta_{k,p} \in \mathbb{T}_R$ the *fast-varying* part of the RIS phase profile and $\zeta_{k,q} \in \mathbb{T}_R^{N_{\text{ris}}}$ the *slow-varying* part. Notice that since \mathbb{T}_R is closed under multiplication, the $\gamma_{k,t}$ in (4) is in $\mathbb{T}_R^{N_{\text{ris}}}$.

While the slow-varying parts are predetermined, we will design the fast varying part such that, for all $k = 1 \dots, K$, $k' \neq k$, we have

$$\sum_{p=0}^{P-1} \beta_{k,p} \beta_{k',p}^* = 0 \text{ and } \sum_{p=0}^{P-1} \beta_{k,p} = 0 \quad (5)$$

$$\beta_{k,p} \in \mathbb{T}_R, \forall k, p. \quad (6)$$

With this design, in the Rx we first multiply the received signal with the conjugate of the transmitted pilot to obtain $\mathbf{w}_t = \mathbf{y}_t$. Then we calculate

$$\mathbf{z}_{k,q} = \sum_{p=0}^{P-1} \beta_{k,p}^* \mathbf{w}_{qP+p} = P \sqrt{E_s} \mathbf{H}_k(\zeta_{k,q}) \mathbf{1}_{N_{\text{tx}}} + \boldsymbol{\nu}_{k,q} \quad (7)$$

$$\mathbf{z}_{0,q} = \sum_{p=0}^{P-1} \mathbf{w}_{qP+p} = P \sqrt{E_s} \mathbf{H}_0 \mathbf{1}_{N_{\text{tx}}} + \boldsymbol{\nu}_{0,q}, \quad (8)$$

where, $\mathbf{1}_{N_{\text{tx}}}$ denotes the all-one vector of length N_{tx} . Vectors $\boldsymbol{\nu}_{k,q}$ and $\boldsymbol{\nu}_{0,q}$ represent the additive noise with distribution $\mathcal{CN}(\mathbf{0}, PN_0 \mathbf{I}_{N_{\text{tx}}})$. It can be seen that in the observations $\mathbf{z}_{k,q}$ all interpath interference is eliminated and that each path can be estimated separately. The question remains how to design the fast-varying part to satisfy (5)–(6), while simultaneously keeping P as small as possible. This will be discussed next.

B. Designing the fast-varying part

In this section, we show how to find a feasible solution of $\beta_{k,p} \in \mathbb{T}_R$ that satisfy (5)–(6) for a given K and R . Also, we consider the problem of finding P^* , the minimum value of P that allows a feasible solution. We refer to such solution as the *optimal solution*. We will now define several concepts, based on which we show for which cases an optimal solution can be found, while providing a simple method for finding a feasible solution for the general case.

We first introduce $\text{BH}(P, R)$ as the set of BH matrices of order P and complexity R , that is all matrices $\boldsymbol{\Upsilon} \in \mathbb{T}_R^{P \times P}$ that satisfy $\boldsymbol{\Upsilon} \boldsymbol{\Upsilon}^H = \mathbf{P} \mathbf{I}_P$, where \mathbf{I}_P is a $P \times P$ identity matrix. In general, these sets may be empty and finding elements in $\text{BH}(P, R)$ or characterizing the entire set is an open problem. However, in [16], a numerical method is introduced to search for BH matrices; the authors publish a list of discovered BH matrices on their Wiki page¹.

Secondly, we represent the prime factorization of R by

$$R = p_1^{e_1} \times p_2^{e_2} \times \cdots \times p_L^{e_L}, \quad (9)$$

where we assume that $p_1 < p_2 < \cdots < p_L$.

Thirdly, we define the vectors $\boldsymbol{\beta}_k = [\beta_{k,0}, \beta_{k,1}, \dots, \beta_{k,P-1}]^T$ and $\boldsymbol{\beta}_0 = \mathbf{1}_P$. Then the conditions (5) can be rewritten as

$$\boldsymbol{\beta}_0 = \mathbf{1}_P \quad (10)$$

$$\boldsymbol{\beta}_k^H \boldsymbol{\beta}_{k'} = P \mathbb{1}(k = k'), \quad (11)$$

¹<https://wiki.aalto.fi/display/Butson>

where $\mathbb{1}(\cdot)$ is the indicator function. Furthermore, we let $\mathbf{B} \in \mathbb{T}_R^{(K+1) \times P}$ be $[\beta_0^\top, \dots, \beta_K^\top]^\top$ and rewrite the conditions (5) as

$$[\mathbf{B}]_1 = \mathbf{1}_P^\top \quad (12)$$

$$\mathbf{B}\mathbf{B}^\mathbf{H} = P\mathbf{I}_{K+1}. \quad (13)$$

C. Special cases

Before dealing with the general case, we consider five specific cases of practical importance for which an optimal solution to (5)–(6) can be found.

1) *Case I: Infinite resolution:* $\beta_{k,p} \in \mathbb{T}$: With infinite phase resolution, we can find a feasible solution by setting β_k^\top to be the k th row of the $P \times P$ discrete Fourier transform (DFT) matrix \mathbf{F}_P , i.e.,

$$\beta_{k,p} = [\mathbf{F}_P]_{k,p} = e^{-j2\pi kd/P}. \quad (14)$$

The condition (11) holds since the DFT matrix is unitary. This also shows, by construction, that $P^* \leq K+1$. Via the following lemma, we prove that the minimum duration solution is $P^* = K+1$.

Lemma 1. *If $P < K+1$, then there is no solution for $\beta_k \in \mathbb{T}_R^P$ that satisfies (11) for $k = 0, \dots, K$.*

Proof. Since $\beta_k \in \mathbb{C}^P$ then, if $K+1 > P$, vectors β_k must be linearly dependent. This is in contradiction to (11). \square

2) *Case II: $p_1 \geq K+1$:* We now show that in this case, $P^* = p_1$. To do so, we first present a solution for β_k with $P = p_1$ and then prove that no solutions exist for $P < p_1$. The first part is done by setting β_k^\top to the k th row of \mathbf{F}_{p_1} . Since $\mathbb{T}_{p_1} \subseteq \mathbb{T}_R$, this yields a valid solution. To prove the second part, we use the following proposition.

Proposition 1. *For any $R > 1$ with the prime factorization (9), let $\mathcal{W}(R)$ be the set of all positive integers M for which there exists $\alpha \in \mathbb{T}_R^M$ such that $\alpha^\top \mathbf{1}_M = 0$. Then*

$$\mathcal{W}(R) = \left\{ \sum_{i=1}^L m_i p_i \mid m_i \in \mathbb{N} \right\} \setminus \{0\}. \quad (15)$$

Proof. See [17]. \square

Now, assume that $P < p_1$ and that $\beta_k \in \mathbb{T}_R^P$ satisfies (10)–(11). Then, $\beta_1^\top \mathbf{1}_P = 0$, which, according to Proposition 1, implies that $P \in \mathcal{W}(R)$. However, from (15), the minimum member of $\mathcal{W}(R)$ is p_1 and this is in contradiction with the assumption that $P < p_1$.

3) *Case III: $R = 2$:* In this case, β_k are real vectors, and therefore we should consider (real) Hadamard matrices in order to find a solution. If $K = 1$, one can check that \mathbf{F}_2 is an optimal solution. For higher values of K , we use the following proposition.

Proposition 2. *If $\text{BH}(P, 2)$ is non-empty, and $P > 2$ then a positive integer κ exists such that $P = 4\kappa$.*

Proof. See [18, Sec. 1.3.2]. \square

The inverse of Proposition 2 reads as follows.

Conjecture 1 (Hadamard Conjecture). *For any positive integer κ , the set $\text{BH}(4\kappa, 2)$ is non-empty.*

This conjecture has been an open problem for over 100 years. However, it has been proven for values $\kappa < 167$ [18], which is enough for most practical purposes. Next, we present the following theorem on optimal solutions for $R = 2$.

Theorem 1. *Let $2 < K < 664$. Then the smallest value of P that yields a solution for $\{\beta_k \in \mathbb{T}_2^P\}_{k=0}^K$ that satisfies (10) and (11) is $P^* = 4\lceil(K+1)/4\rceil$.*

Proof. See Appendix A. \square

To generate the optimal solution one should assign β_k (for $k = 0, \dots, K$) to the k th row of a matrix $\text{BH}(P^*, 2)$ that satisfies (12).

4) *Case IV: $R = 2^r$ with $r > 1$:* We begin by stating a conjecture about the existence of $\text{BH}(P, 4)$ matrices [19].

Conjecture 2. *For all positive integers κ , the set $\text{BH}(2\kappa, 4)$ is non-empty.*

It was shown that this conjecture is true for all $\kappa \leq 32$ [19], which is large enough for all the practical cases that we consider in this paper. The following corollary follows from the fact that for all $r \geq 2$ we have that $\text{BH}(P, 4) \subseteq \text{BH}(P, 2^r)$.

Corollary 1. *For all positive integers $\kappa \leq 32$ and $r \geq 2$, the set $\text{BH}(2\kappa, 2^r)$ is non-empty.*

Next, in the following theorem we discuss the optimal solution.

Theorem 2. *Let $1 \leq K < 64$ and $r \geq 2$, then the smallest value of P , for which there exists a solution for $\{\beta_k \in \mathbb{T}_{2^r}^P\}_{k=0}^K$ that satisfies (10) and (11) is $P^* = 2\lceil(K+1)/2\rceil$.*

Proof. See Appendix B. \square

The optimal solution can be generated based on the rows of a $\text{BH}(P^*, 2^r)$ matrix satisfying (12).

5) *Case V: $\text{BH}(K+1, R)$ is non-empty:* We first introduce the following lemma from [20] for later use.

Lemma 2. *If there exists $\mathbf{G} \in \mathbb{T}_R^{(K+1) \times P}$ that satisfies (13), then there exists a matrix $\mathbf{B} \in \mathbb{T}_R^{(K+1) \times P}$ that satisfies both (12) and (13) and it can be generated as $\mathbf{G}\mathbf{A}^\mathbf{H}$, where $\mathbf{A} = \text{diag}([\mathbf{G}]_1)$.*

Proof. The proof follows by simply substituting \mathbf{B} into (12) and (13). \square

Let now $\mathbf{A} \in \text{BH}(K+1, R)$. Then by using Lemma 2 we can generate matrix \mathbf{B} whose rows represent a solution for β_k in \mathbb{T}_B^{K+1} . Therefore, we have that $P^* \leq K+1$. However, based on Lemma 1, we have $P^* \geq K+1$, and thus $P^* = K+1$.

D. General case

We note that based on Lemma 2, we can relax the condition (12) and only search for matrices $\mathbf{B} \in \mathbb{T}_R^{(K+1) \times P}$ that satisfies (13). We call the set of such matrices partial BH (PBH) matrices of order $(K+1, P)$ and complexity R and denote it by $\text{PBH}(K+1, P, R)$. It is evident that $\text{PBH}(P, P, R) =$

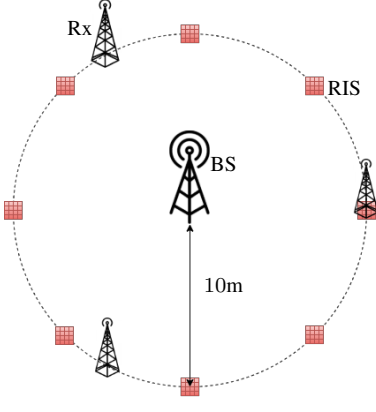


Figure 1. System setup with 8 RISs and three Rxs located on a circle of radius 10 m around the BS. The RISs and Rxs are on $z = -3$ m and $z = 1$ m planes, respectively and BS is at origin.

$\text{BH}(P, R)$. Thus, since finding BH matrices, in general, is an open problem, so is finding PBH ones. One way to generate a $\text{PBH}(K+1, P, R)$ is by selecting the first $K+1$ rows of a $\text{BH}(P, R)$ matrix with $P \geq K+1$. In what follows we present a simple method to generate this BH matrix using the DFT matrices.

We define the set

$$\mathcal{V}(R) = \left\{ \prod_{i=1}^L p_i^{m_i} \geq K+1 \mid m_i \in \mathbb{N} \right\} \quad (16)$$

and determine $\tilde{v} = \min\{\mathcal{V}(R)\} = \prod_{i=1}^L p_i^{\tilde{m}_i}$. Then $\mathbf{S} = \mathbf{F}_{p_1}^{\otimes \tilde{m}_1} \otimes \dots \otimes \mathbf{F}_{p_L}^{\otimes \tilde{m}_L}$ is a $\text{BH}(\tilde{v}, R)$ matrix that satisfies (12). Therefore, one can set β_k^\top to the first $K+1$ rows of \mathbf{S} . In general, this solution may not be optimal. However, if $p_1 \geq K+1$ then $\mathbf{S} = \mathbf{F}_{p_1}$, which, as proved in Sec. III-C2, is the optimal solution.

E. Summary

We have shown for 5 special cases that optimal solutions can be found and provided a method to find such solution. For the general case, we can only provide a constructive method for finding feasible solutions, though without guarantee of optimality.

IV. SIMULATION RESULTS

In this section, we illustrate the effectiveness of the proposed method in mitigating the interpath interference in a semi-passive localization scenario from [13].

A. Scenario

In this setup we consider $K = 8$ RISs, one base station (BS) transmitting pilot signals, and 3 receivers that receive the signal directly from the BS and also the reflected signal from the RISs. The placement of each of the elements is depicted in Fig. 1. We consider the transmission of orthogonal frequency-division multiplexing (OFDM) signals from the BS. The parameters of the signal and noise can be found in [13, Table I]. We set $Q = 1$ and select $\zeta_{k,0}$ randomly. We then

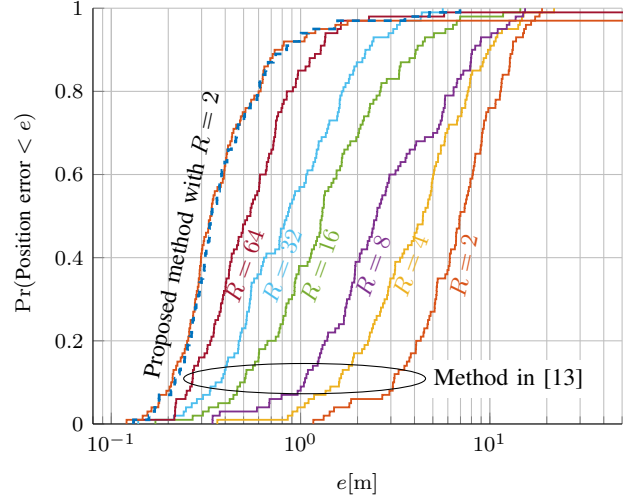


Figure 2. Cumulative distribution of root mean squared error (e in meter) of the estimator over 100 random realizations of RIS phase profiles. The results are presented for our method with one-bit RIS phase resolution ($R = 2$) and for the method in [13], followed by quantization with $R \in \{1, 4, \dots, 64\}$. The theoretical lower bound is shown by the dashed line.

estimate the location of each of the K RISs as follows. We first resolve the interpath interference at each Rx via orthogonal coding of the RIS phase profiles as described in Section III. Then, we calculate the time-of-arrival (ToA) of all the $K+1$ paths arriving at each of the Rxs (see [13, Sec. III-B]). Finally, we estimate the RIS location based on the calculated ToAs (see [13, III-C]).

B. Fast-varying phase profiles

With regard to the fast-varying part of the RIS phase profile (i.e., β_k), we consider two different methods:

- **Proposed method:** The first method is based on our proposal in Section III-B, where we assume that RISs have one bit of phase resolution (i.e., $R = 2$). Based on our results in Section III-C3 we set $P = 12$ and we let β_k be the rows of a $\text{BH}(2, 12)$ matrix (or equivalently, a 12×12 Hadamard matrix).
- **Benchmark:** With the second method, we ignore the limited phase resolution and design β_k as in Sec. III-C1 and [13]. For a fair comparison, we consider the same number of transmission as in the proposed method, i.e., $P = 12$. Therefore, we set β_k to be the rows of the matrix \mathbf{F}_{12} . We consider six different phase resolutions $R \in \{2, 4, 8, 16, 32, 64\}$. For each R , we map the values of $\beta_{k,p}$ (obtained from \mathbf{F}_{12}) to the closest point in \mathbb{T}_R to account for limited phase resolution of the RISs. Such quantization impairs the orthogonality of β_k . Therefore, we expect that the estimator cannot avoid interpath interference and its accuracy deteriorates.

C. Results and discussion

In Fig. 2, we demonstrate the cumulative distribution function (CDF) of the RIS position estimation error for 100 random realizations of $\zeta_{k,0} \in \mathbb{T}_R^{N_{\text{ris}}}$. We present the results for the

RIS located at $(10, 0, -3)$. As it can be seen, the performance degradation due to quantization is more severe with low values of R . On the other hand, our method takes into account the limited resolution of the RIS phase shifts and therefore, avoids any quantization effects. It can be seen that via our proposed method, with only one-bit resolution, the estimator can attain the theoretical lower bound, which is calculated through Fisher information matrix (FIM) analysis [21, Chapter 3].

V. CONCLUSION

We proposed a method to resolve interpath interference in wireless systems equipped with multiple RISs with limited phase resolution. We did so by dividing the RIS phase profiles into a fast-varying and a slow-varying part and designing the former part to be orthogonal across RISs. We proposed a method to find such orthogonal sequences in general and discussed the special cases where such sequences are optimal (have the shortest length). Our solution can be applied to most system models considered in the literature. Future work can explore a trade-off between the interpath interference and number of transmissions (P) and look for sequences $(\beta_k \in \mathbb{T}_R^P)$ with minimum correlation for a given P .

APPENDIX A PROOF OF THEOREM 1

Let $U = 4\lceil(K+1)/4\rceil$ and P^* be the smallest value of P that yields a solution. From Conjecture 1 and Lemma 2, we know that matrix \mathbf{B} exists such that $\mathbf{B} \in \text{BH}(U, 2)$ and $[\mathbf{B}]_1$ satisfies (10). Therefore, the first $K+1$ rows of \mathbf{B} provide a solution for β_k (note that the dimension of \mathbf{B} is at least $K+1$). Furthermore, from Lemma 1 we know that $P^* \geq K+1$. To complete the proof, we need to show that any P that yields a solution for β_k must be a factor of 4. The proof is in the same lines as the proof of Proposition 2 in [18, Sec. 1.3.2] and we present it here for completeness.

Based on (10) and (11), we have that $\beta_2^\top \mathbf{1}_P = 0$, therefore, P should be even and β_2 contain equal number of 1 and -1 . Without loss of generality we can assume that $\beta_2 = [\mathbf{1}_{P/2}^\top, -\mathbf{1}_{P/2}^\top]$. Then since $\beta_3^\top \beta_2 = 0$ we have that $\Sigma_1 - \Sigma_2 = 0$, where Σ_1 (Σ_2) is the summation of all the elements in the first (second) half of vector β_3 . Furthermore, since $\beta_3^\top \beta_1 = 0$, we get $\Sigma_1 + \Sigma_2 = 0$. Therefore, we have $\Sigma_1 = \Sigma_2 = 0$ which proves that each half of the vector β_3 must contain equal number of 1 and -1 . Therefore, the length of β_3 , which is P , must be divisible by 4.

APPENDIX B PROOF OF THEOREM 2

Let $U = 2\lceil(K+1)/2\rceil$ and P^* be the smallest value of P that yields a solution. Based on Corollary 1 and Lemma 2, there exists $\mathbf{B} \in \text{BH}(U, 2^r)$ whose first $K+1$ rows determine a solution for $\{\beta_k \in \mathbb{T}_{2^r}^P\}_{k=0}^K$ (note that $U \geq K+1$). Therefore, $P^* \leq U$. Furthermore, from (10) and (11), we have that $\beta_1^\top \mathbf{1}_{P^*} = 0$. Therefore, from Proposition 1 we have that $P^* \in \mathcal{W}(2^r)$, which is the set of positive even numbers (see (15)). Also, from Lemma 1 we know that $P^* \geq K+1$. Therefore, P^* must be larger than or equal to the smallest even number larger than $K+1$, that is U .

REFERENCES

- [1] E. Björnson, H. Wymeersch *et al.*, "Reconfigurable intelligent surfaces: A signal processing perspective with wireless applications," *arXiv preprint arXiv:2102.00742*, 2021.
- [2] A. Abrardo, D. Dardari, and M. Di Renzo, "Intelligent reflecting surfaces: Sum-rate optimization based on statistical CSI," *arXiv preprint arXiv:2012.10679*, 2020.
- [3] Q. Wu, S. Zhang *et al.*, "Intelligent reflecting surface aided wireless communications: A tutorial," *IEEE Transactions on Communications*, 2021.
- [4] C. Pan, H. Ren *et al.*, "Reconfigurable intelligent surfaces for 6g systems: Principles, applications, and research directions," *IEEE Commun. Magazine*, 2021.
- [5] M. Di Renzo, A. Zappone *et al.*, "Smart radio environments empowered by reconfigurable intelligent surfaces: How it works, state of research, and the road ahead," *IEEE J. Select. Areas Commun.*, vol. 38, no. 11, pp. 2450–2525, 2020.
- [6] G. C. Alexandropoulos and E. Vlachos, "A hardware architecture for reconfigurable intelligent surfaces with minimal active elements for explicit channel estimation," in *Int. Conf. Acoust. Speech Signal Process. (ICASSP)*, 2020, pp. 9175–9179.
- [7] D. Mishra and H. Johansson, "Channel estimation and low-complexity beamforming design for passive intelligent surface assisted MISO wireless energy transfer," in *Int. Conf. Acoust. Speech Signal Process. (ICASSP)*, 2019, pp. 4659–4663.
- [8] T. L. Jensen and E. De Carvalho, "An optimal channel estimation scheme for intelligent reflecting surfaces based on a minimum variance unbiased estimator," in *Int. Conf. Acoust. Speech Signal Process. (ICASSP)*, 2020, pp. 5000–5004.
- [9] C. You, B. Zheng, and R. Zhang, "Channel estimation and passive beamforming for intelligent reflecting surface: Discrete phase shift and progressive refinement," *IEEE J. Select. Areas Commun.*, vol. 38, no. 11, pp. 2604–2620, 2020.
- [10] B. Ning, Z. Chen *et al.*, "Channel estimation and transmission for intelligent reflecting surface assisted THz communications," in *IEEE Int. Conf. Commun. (ICC)*. IEEE, 2020.
- [11] G. C. Alexandropoulos, S. Samarakoon *et al.*, "Phase configuration learning in wireless networks with multiple reconfigurable intelligent surfaces," in *IEEE Global Commun. Conf. (GLOBECOM)*, 2020.
- [12] W. Wang and W. Zhang, "Joint beam training and positioning for intelligent reflecting surfaces assisted millimeter wave communications," *IEEE Trans. Wireless Commun.*, Apr. 2021.
- [13] K. Keykhosravi, M. F. Keskin *et al.*, "Semi-passive 3D positioning of multiple RIS-enabled users," *arXiv preprint arXiv:2104.12113*, 2021.
- [14] A. Elzanaty, A. Guerra *et al.*, "Reconfigurable intelligent surfaces for localization: Position and orientation error bounds," *arXiv preprint arXiv:2009.02818*, 2020.
- [15] K. Keykhosravi, M. F. Keskin *et al.*, "SISO RIS-enabled joint 3D downlink localization and synchronization," in *IEEE Int. Conf. Commun. (ICC)*, 2021.
- [16] P. Lampio, P. Östergård, and F. Szöllösi, "Orderly generation of Butson Hadamard matrices," *Mathematics of Computation*, vol. 89, no. 321, pp. 313–331, 2020.
- [17] T. Y. Lam and K. H. Leung, "On vanishing sums of roots of unity," *J. algebra*, vol. 224, no. 1, pp. 91–109, Feb. 2000.
- [18] A. J. LaClair, "A survey on Hadamard matrices," 2016.
- [19] J. Seberry, "Complex Hadamard matrices," 1973.
- [20] A. Butson, "Generalized Hadamard matrices," *Proceedings of the American Mathematical Society*, vol. 13, no. 6, pp. 894–898, 1962.
- [21] S. M. Kay, *Fundamentals of statistical signal processing: Estimation Theory*. Prentice Hall PTR, 1993.